Supplementary Information

The monoiron anion, *fac*-$[Fe(CO)_3I_3]^-$ and its organic aminium salts: their preparation, CO-release and cytotoxicity

Xiuqin Yang,‡[a,b] Jing Jin,‡[c] Zhuming Guo,[d] Zhiyin Xiao,*[a] Naiwen Chen,[c] Xiujuan Jiang,[a] Yi He,*[c] and Xiaoming Liu*[a]

[a] College of Biological, Chemical Sciences and Engineering, Jiaxing University, Jiaxing 314001, China

[b] College of Chemistry and Life Sciences, Zhejiang Normal University, Jinhua 321004, China

[c] Department of Urology, The Affiliated Hospital of Jiaxing University, Jiaxing 314001, China

[d] College of Chemistry and Bioengineering, Guilin University of Technology, Guilin, 514006, China

‡ These authors have equal contribution towards this work.

Email: xiaoming.liu@mail.zjxu.edu.cn (X. Liu); zhiyin.xiao@zjxu.edu.cn (Z. Xiao); heyi@zjxu.edu.cn (Y. He)

Tel./Fax: +86 (0)573 83643937

Contents

the present of NaI (0.24 mol L^{-1}) and (b) plot of the vibrational absorption (2090 cm^{-1}) of salt **5** against the process time in D_2O solvent.

Figure S19 (a) Infrared spectral variation during the CO-releasing process of salt **5** in the present of glucose (0.1 mol L^{-1}) and (b) plot of the vibrational absorption (2090 cm^{-1}) of salt **5** against the process time in D_2O solvent.

Figure S20 Infrared spectral variation during the CO-releasing process of salt **5** in D_2O solvent under N_2 atmosphere in dark.

Figure S21 Mass spectra of i-CORM's solution of salt **5** in D_2O solvent.

Figure S22 nonlinear regression results of viabilities of RT112 against their responded Logarithm of salt's concentration (log *c*) to estimate IC_{50} values of **1** (a), **2** (b), **3**(c), **4** (d) and **5** (e) in 24 h, respectively.

Figure S23 nonlinear regression results of viabilities of RT112 against their responded Logarithm of the i-CORMs' concentration (log *c*) derived from salt **5** to estimate its IC_{50} value in 24 h.

Figure S24 nonlinear regression results of viabilities of SV-HUC-1 against their responded Logarithm of salt's concentration (log *c*) to estimate IC_{50} values of **1** (a), **2**(b), **3** (c), **4** (d) and **5** (e) in 24 h, respectively.

Table S1 Crystal data and structural refinements for salts **1–4**.

Table S2 Selected bond lengths (Å) and angles (°) for salts **1–4**.

.

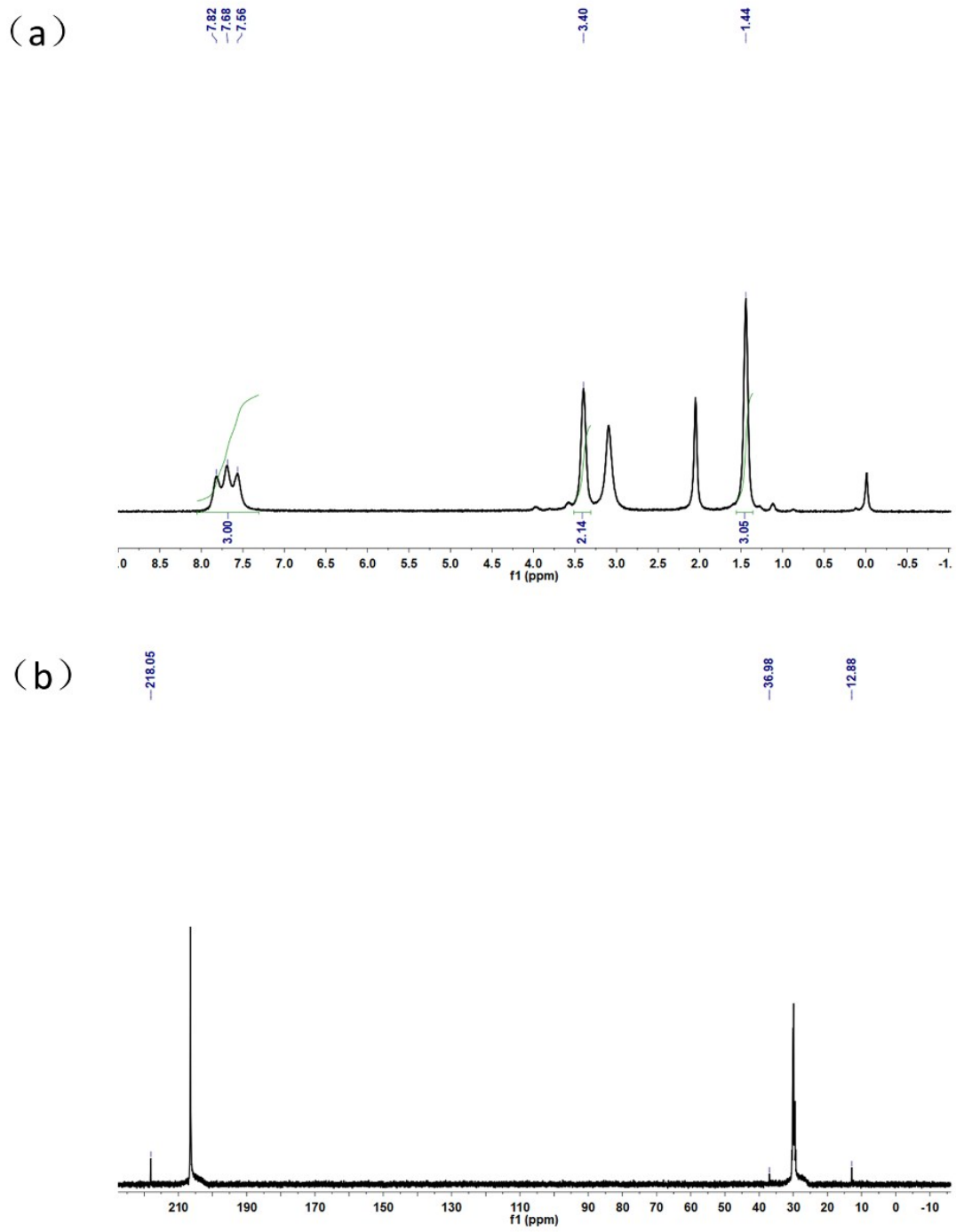

Figure S1 ^{1}H / ^{13}C NMR spectra of salt **1** in acetone-d^6 solvent.

（a）

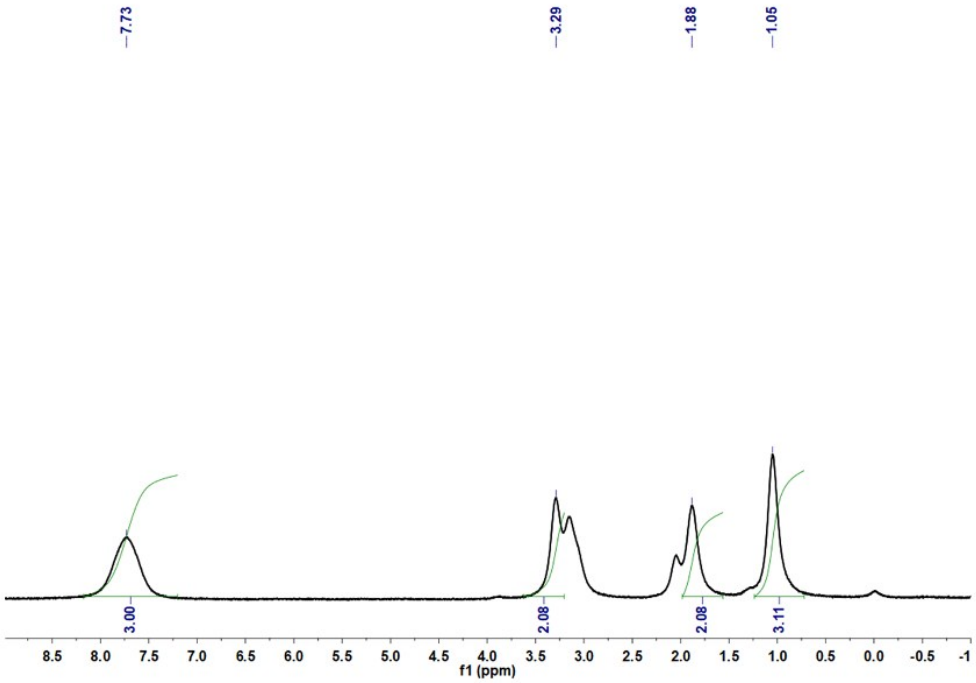

（b）

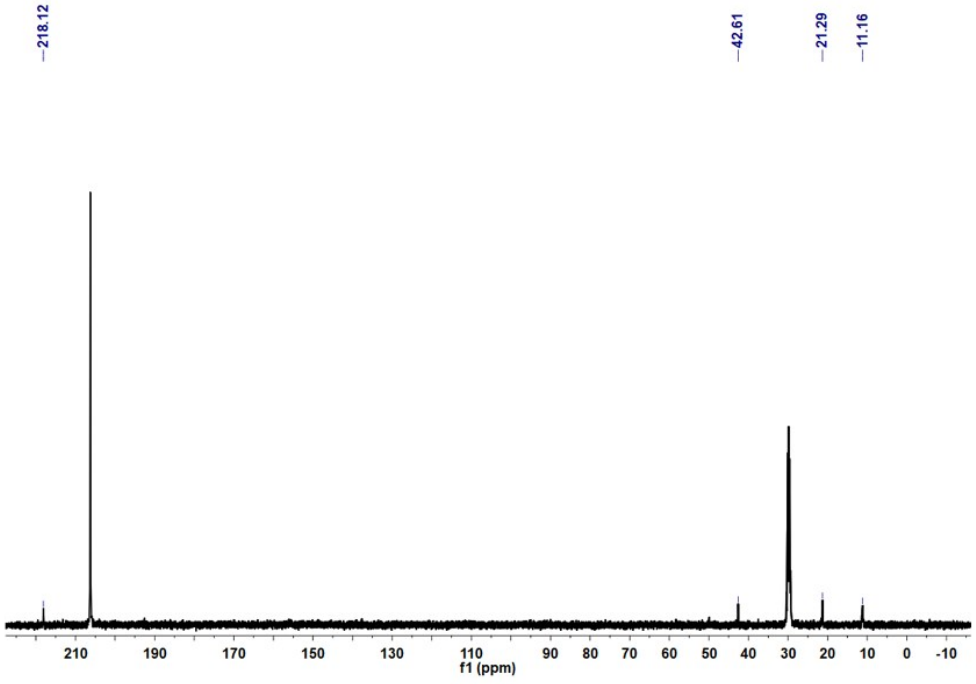

Figure S2 ^{1}H / ^{13}C NMR spectra of salt **2** in acetone-d^6 solvent.

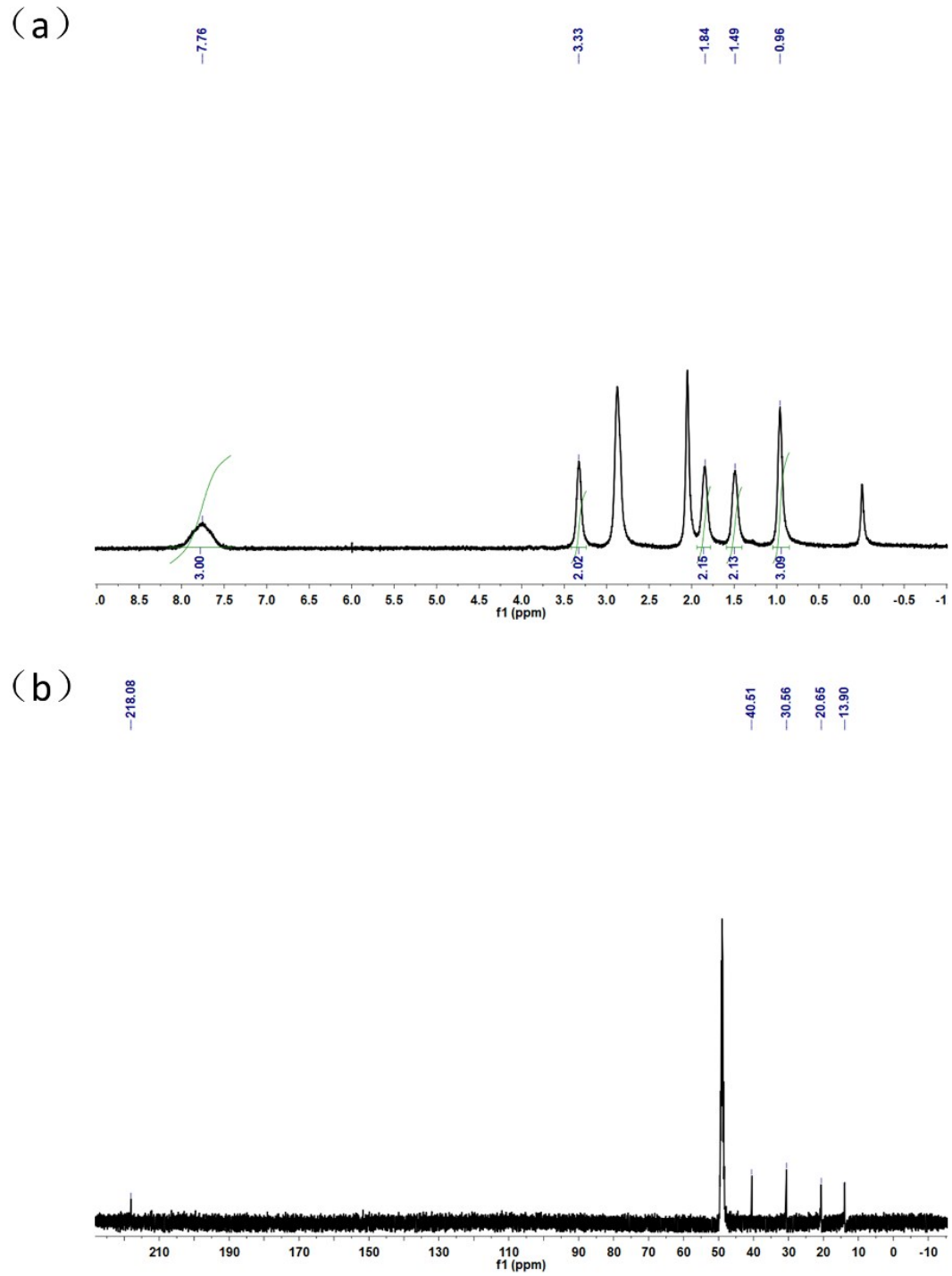

Figure S3 ^{1}H / ^{13}C NMR spectra of salt **3** in acetone-d^6 solvent.

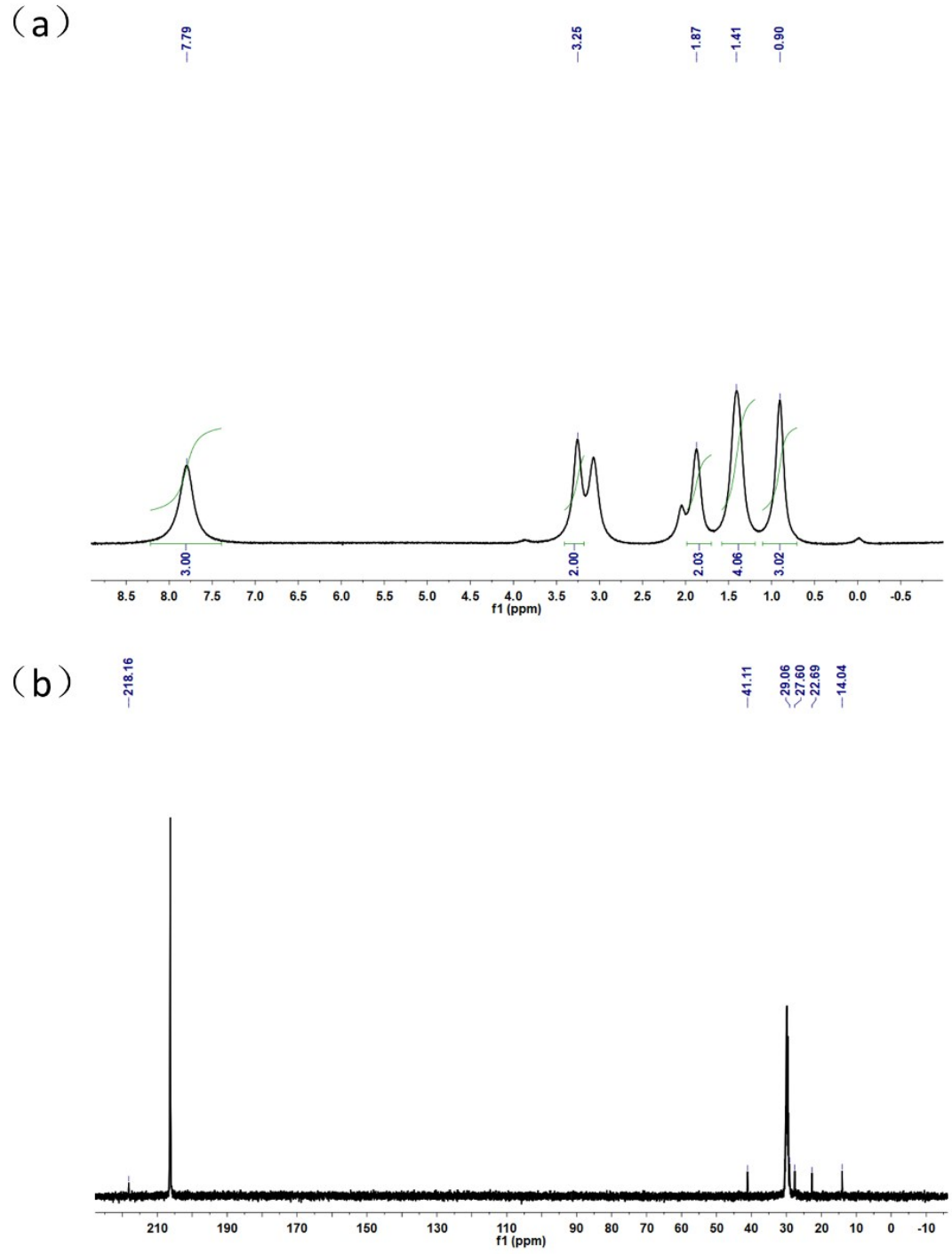

Figure S4 ^{1}H / ^{13}C NMR spectra of salt **4** in acetone-d^{6} solvent.

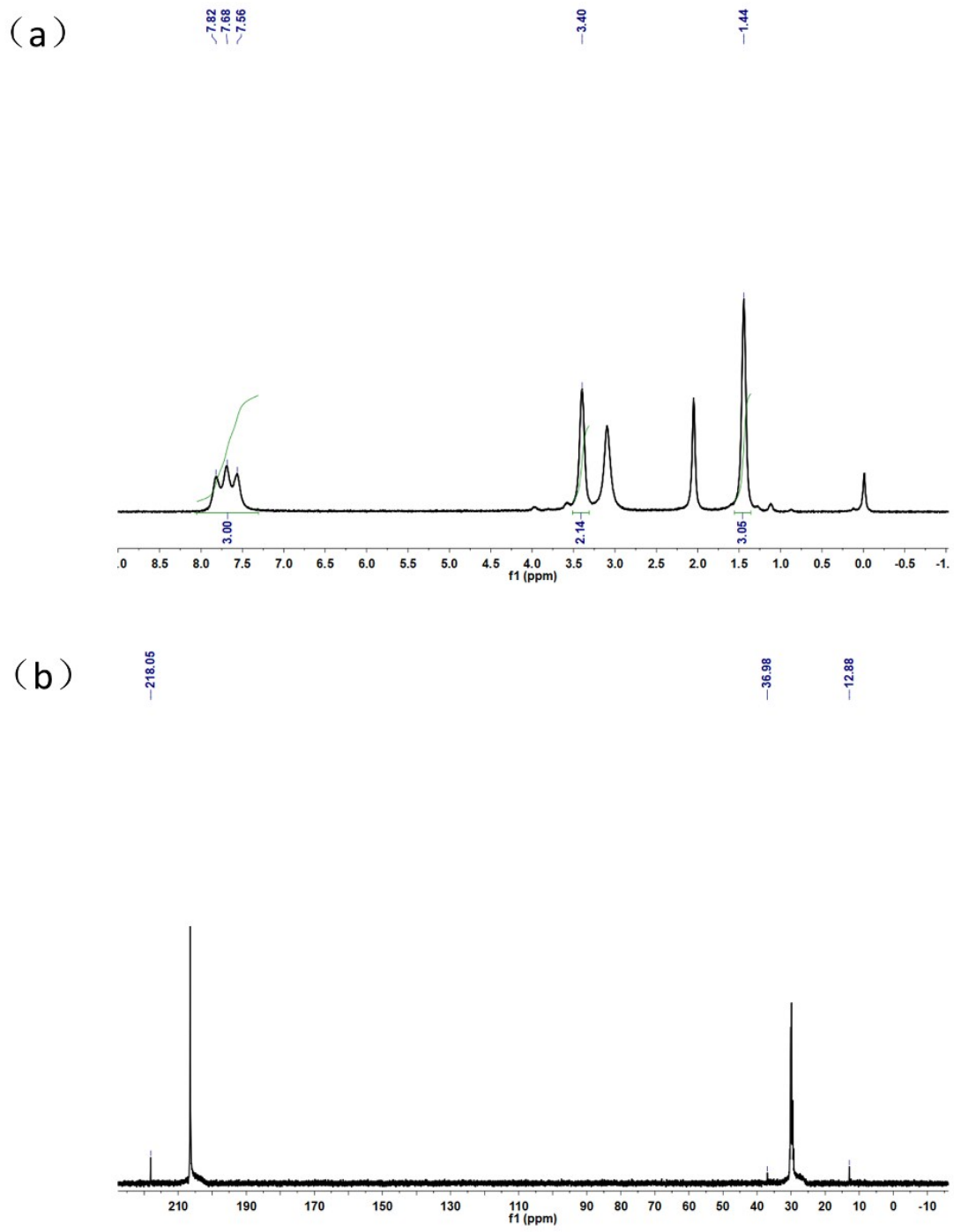

Figure S5 ^{1}H / ^{13}C NMR spectra of salt **5** in acetone-d^6 solvent.

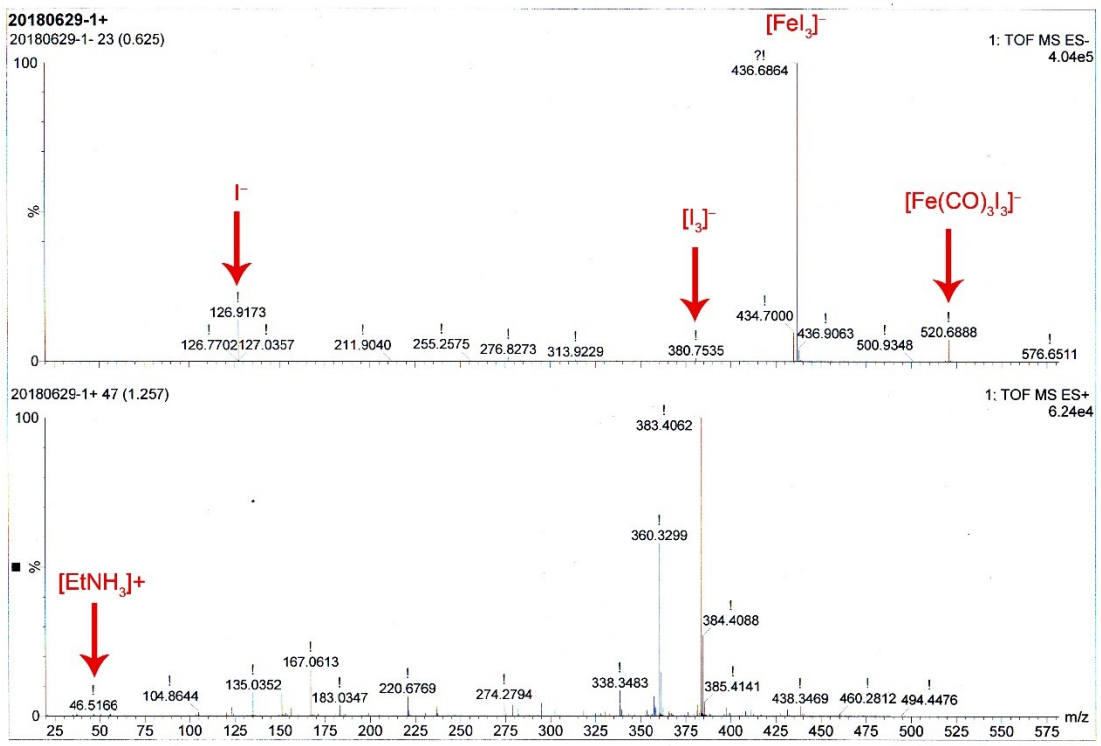

Figure S6 Mass spectra of salt **1** in MeOH.

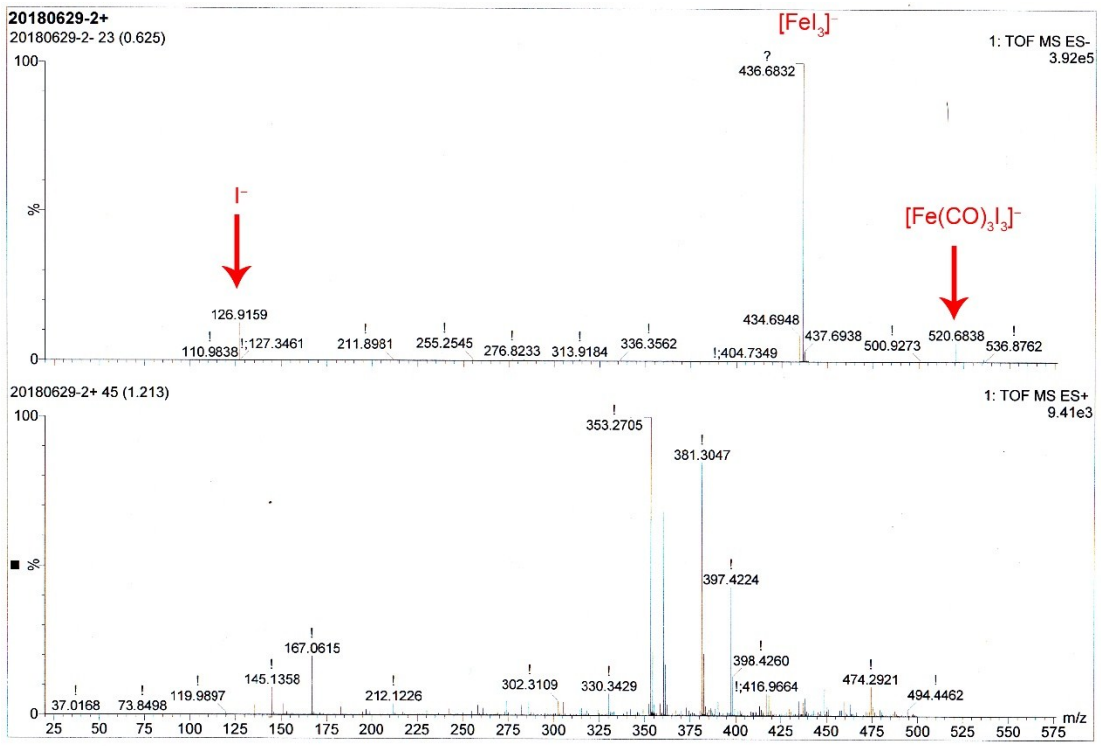

Figure S7 Mass spectra of salt **2** in MeOH

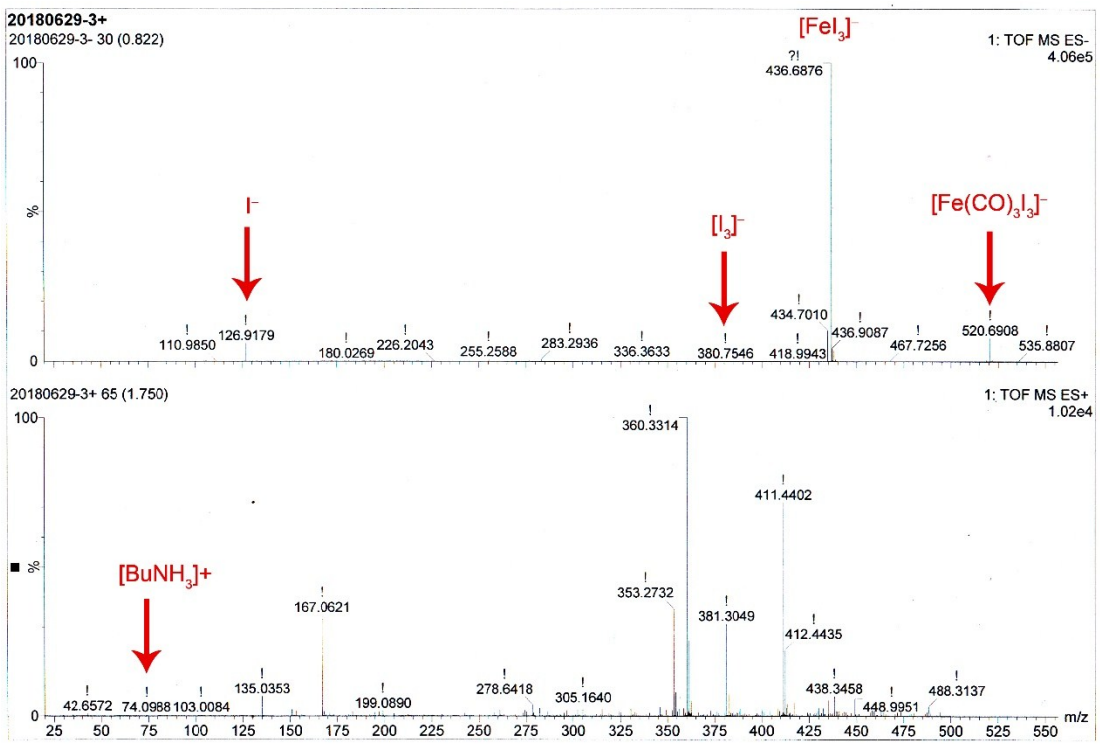

Figure S8 Mass spectra of salt **3** in MeOH.

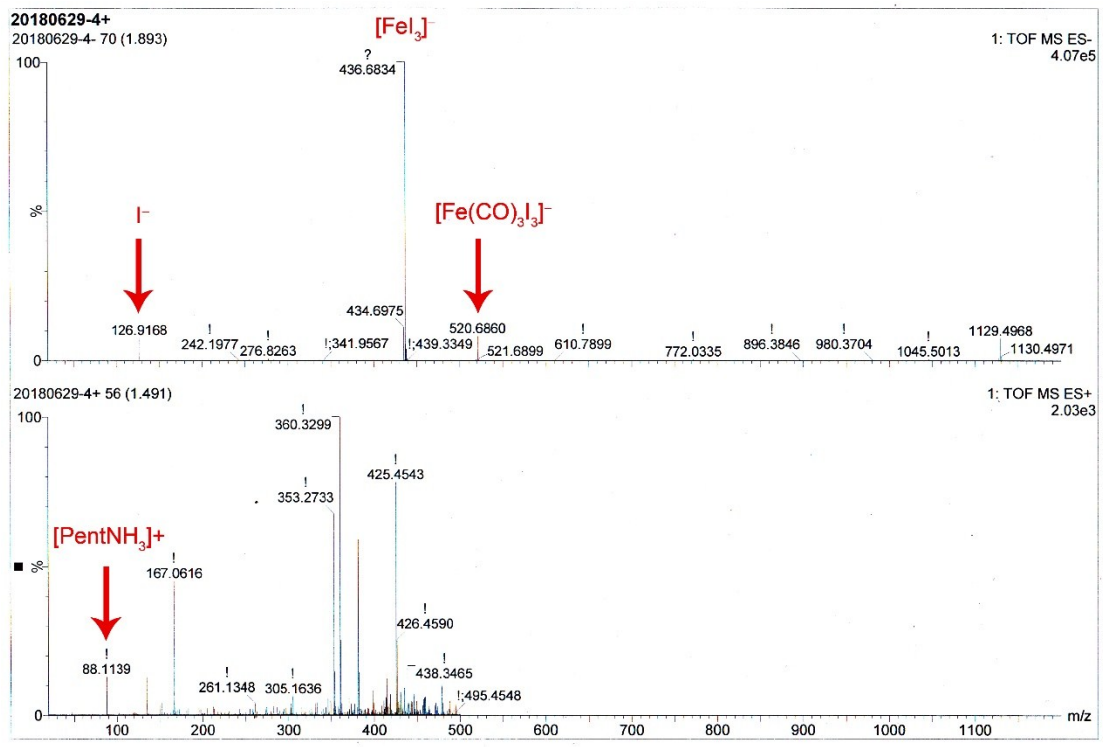

Figure S9 Mass spectra of salt **4** in MeOH.

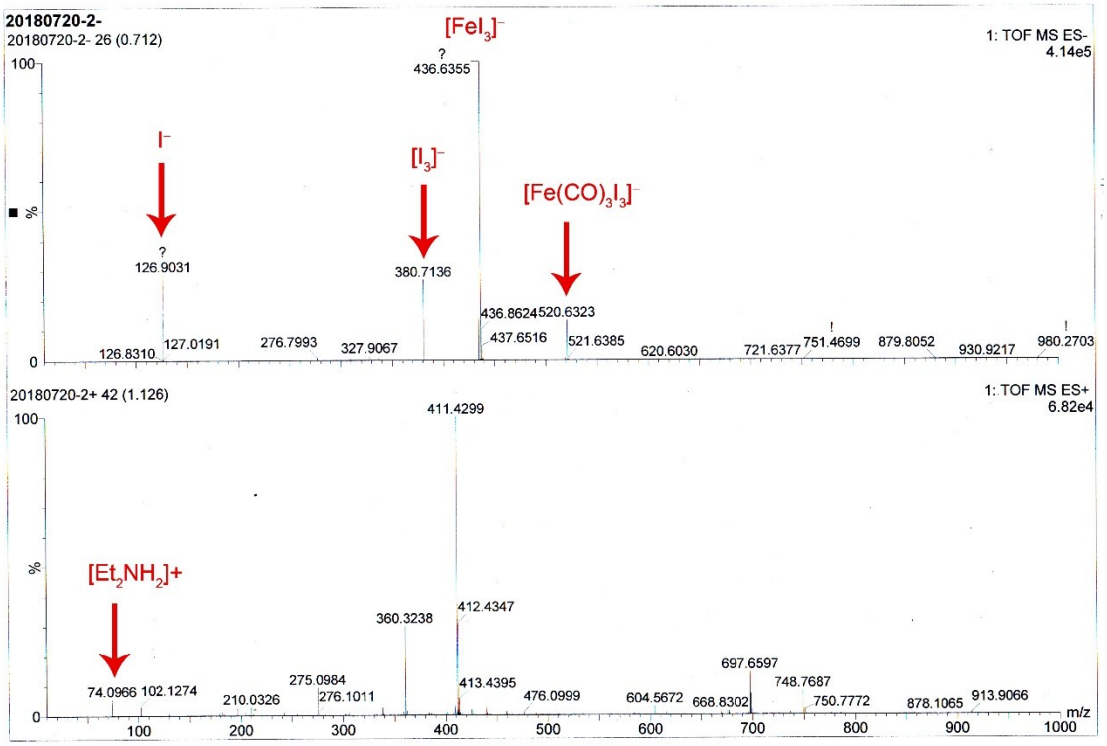

Figure S10 Mass spectra of salt **5** in MeOH.

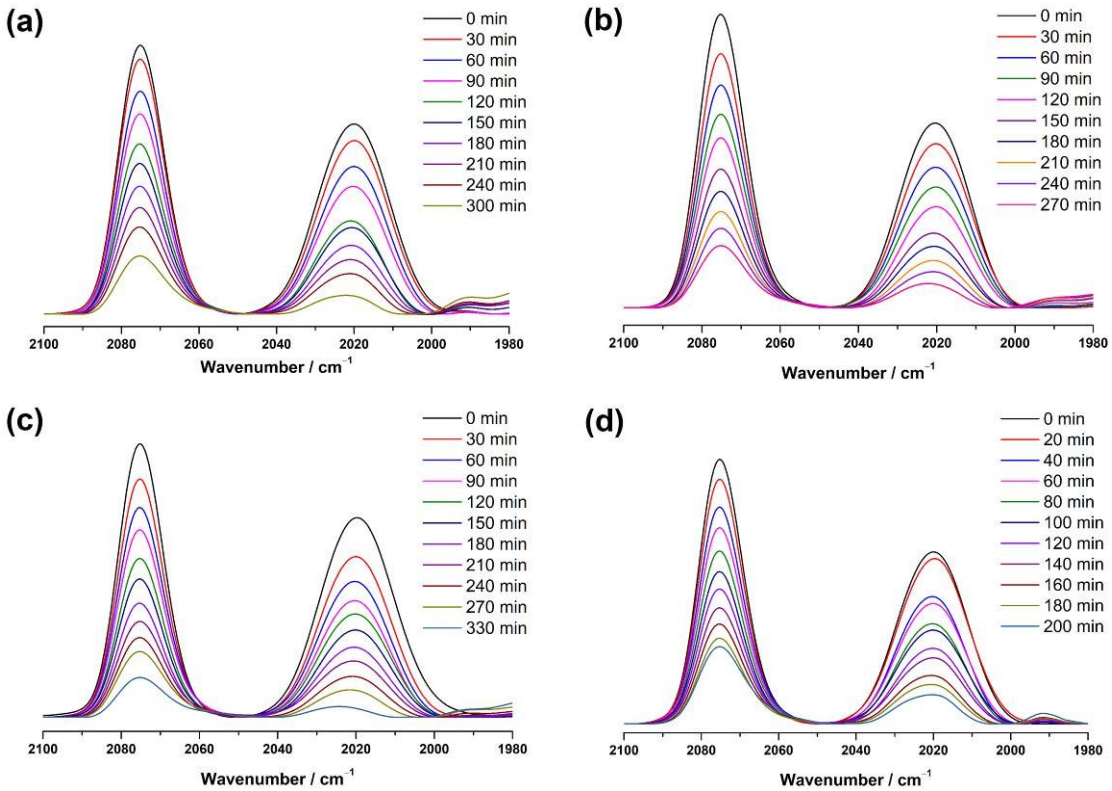

Figure S11 Infrared spectral variation during the CO-releasing process of salts **2** (a), **3** (b) and **4** (c), and **5** (d) in DMSO with a concentration of 0.008 mol L^{-1} at 37 °C under an open atmosphere in dark, respectively.

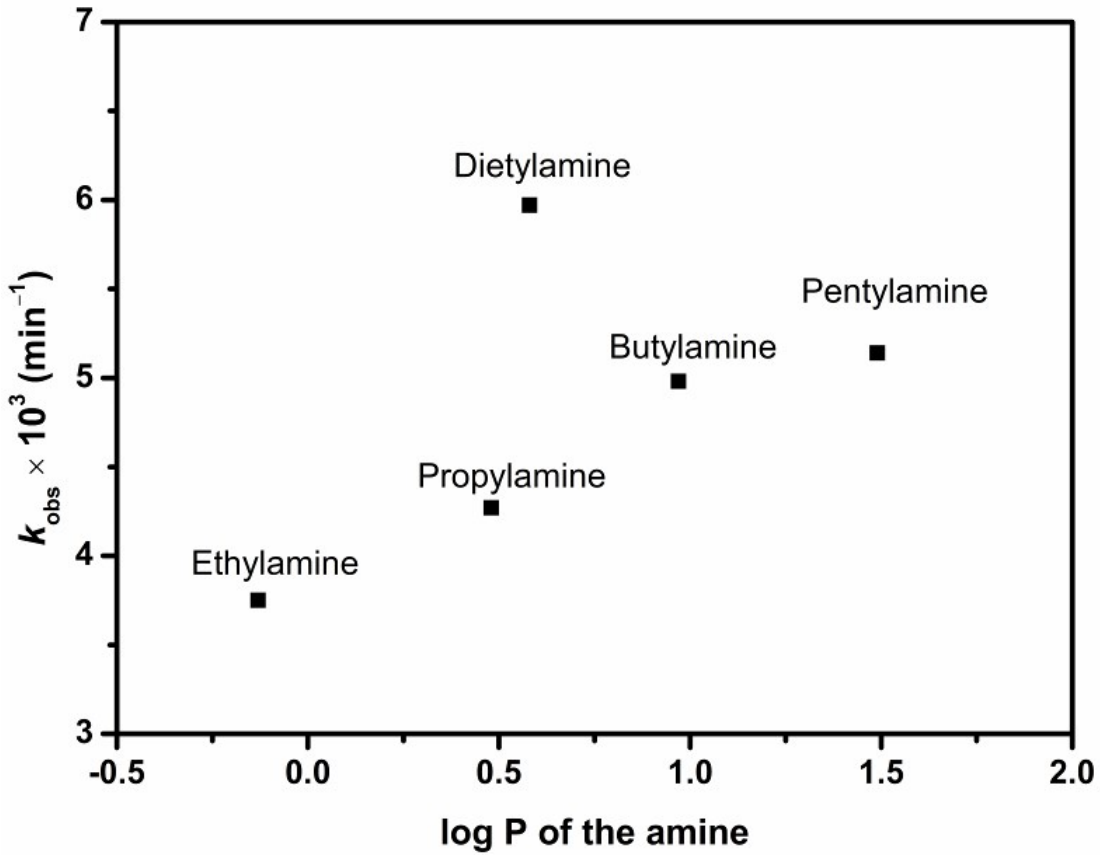

Figure S12 Plot of rate constant (k_{obs}) of the salts in DMSO against the logarithm of the octanol/water partition coefficient (log P) of the amines.

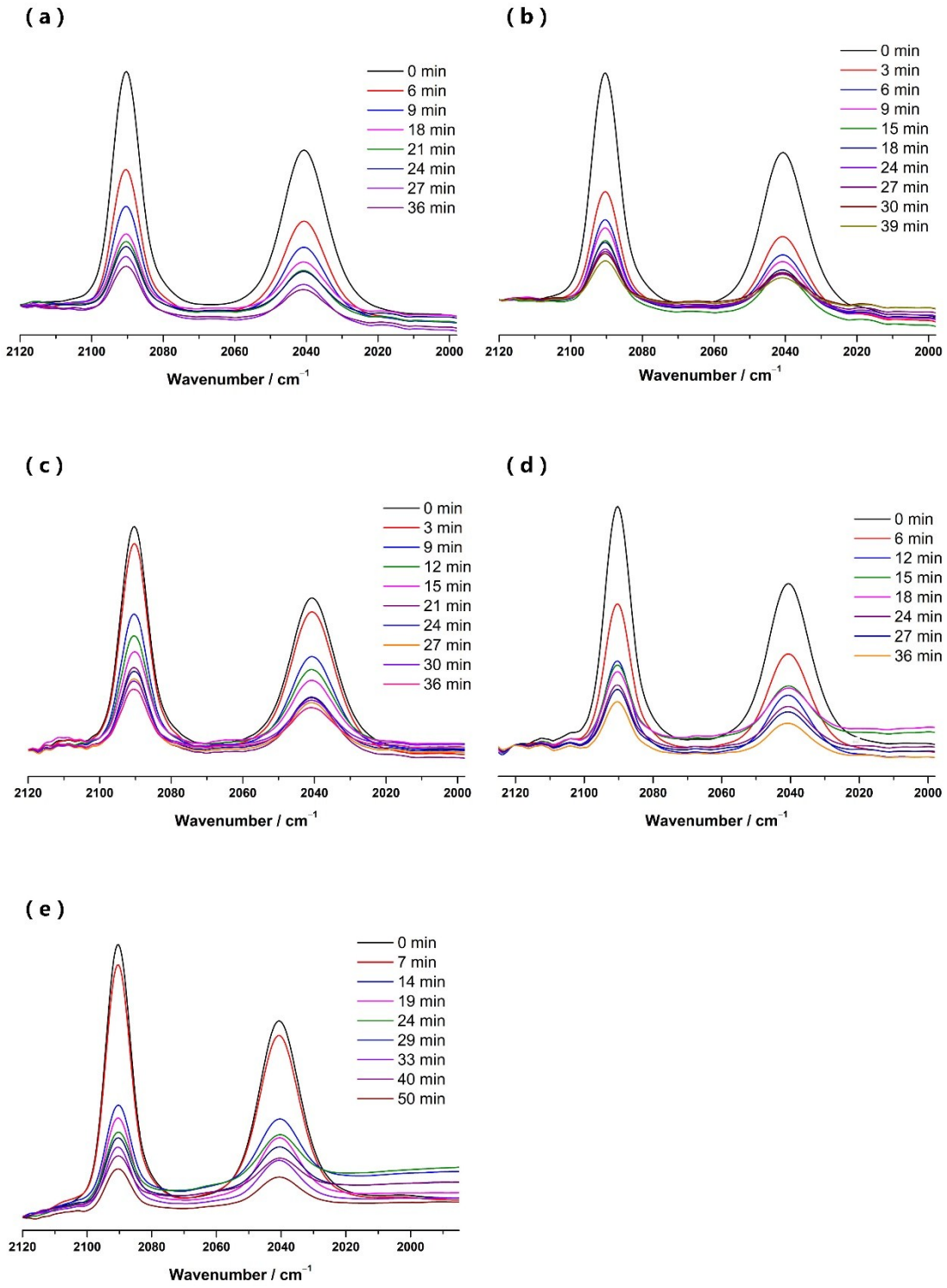

Figure S13 Infrared spectral variation during the CO-releasing process of salts **1** (a), **2** (b), **3** (c), **4** (d), and **5** (e) in D_2O with a concentration of 8.0 mmol L^{-1} at 37 ^{o}C under an open atmosphere in dark, respectively.

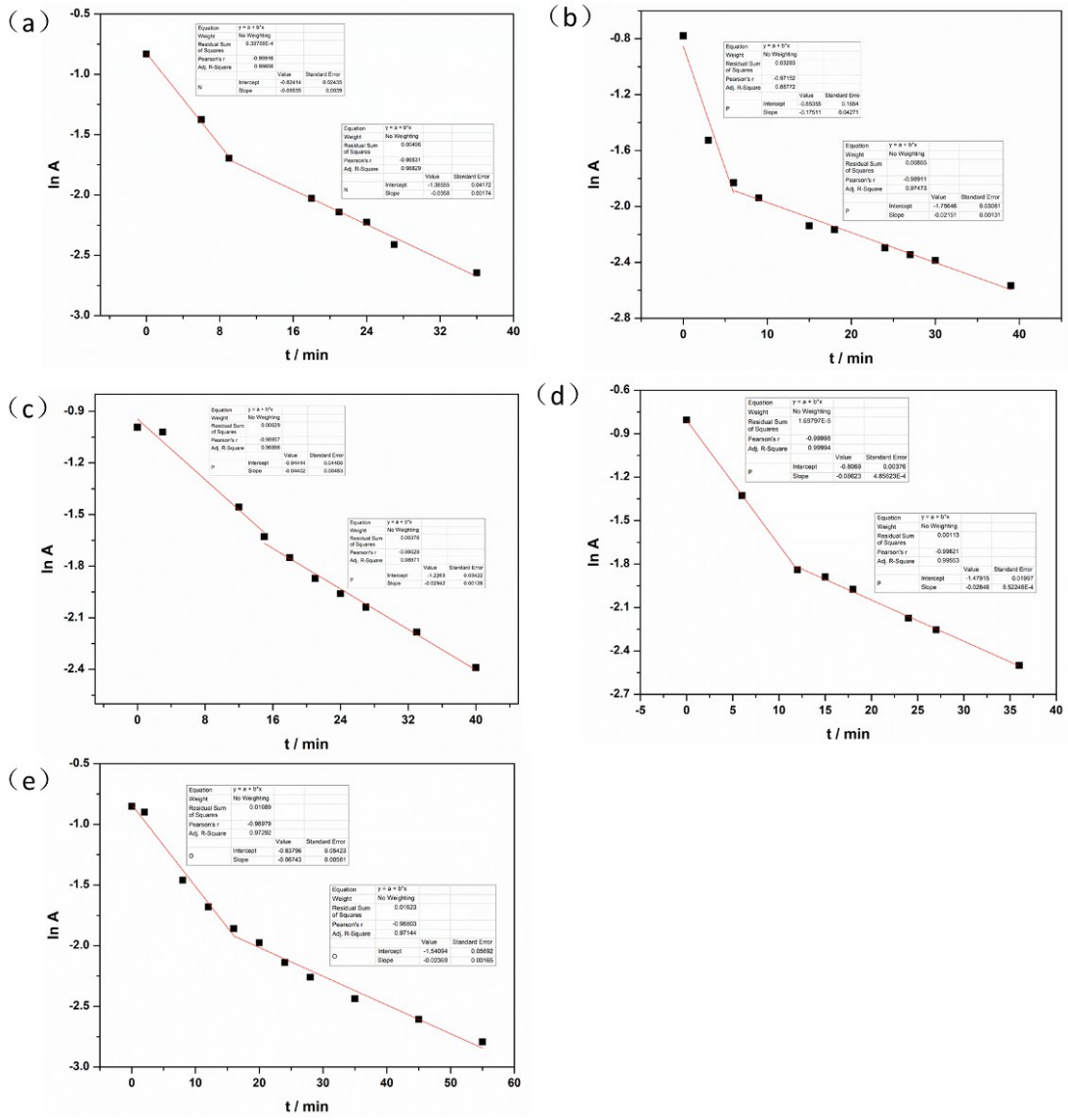

Figure S14 Plots of the vibrational absorption (2090 cm^{-1}) of salts **1** (a), **2** (b), **3** (c), **4** (d), and **5** (e) against the process time in D_2O solvent (conditions: 8.0 mmol L^{-1} / 37 ^oC / open air / dark).

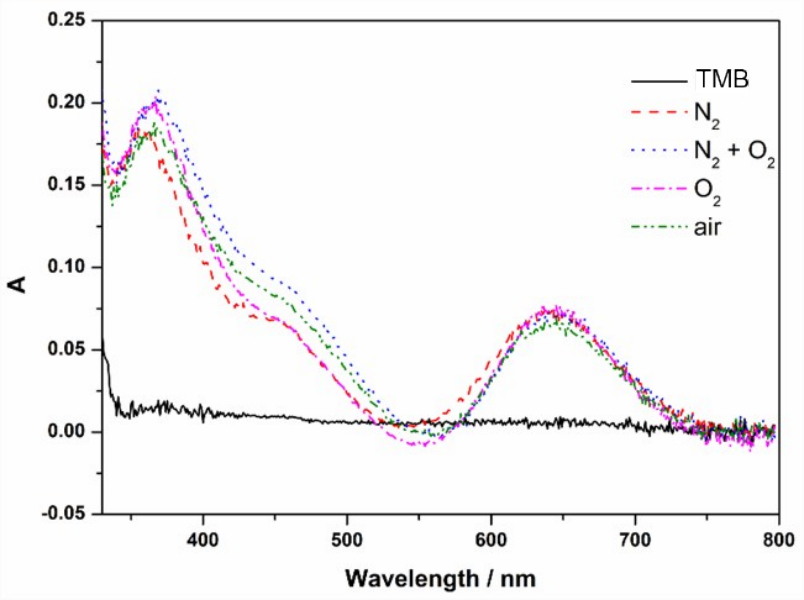

Figure S15 UV-vis spectra of TMB in HOAc-NaOAc buffer (pH = 4.5) with the presence of salt **5** under different atmospheres.

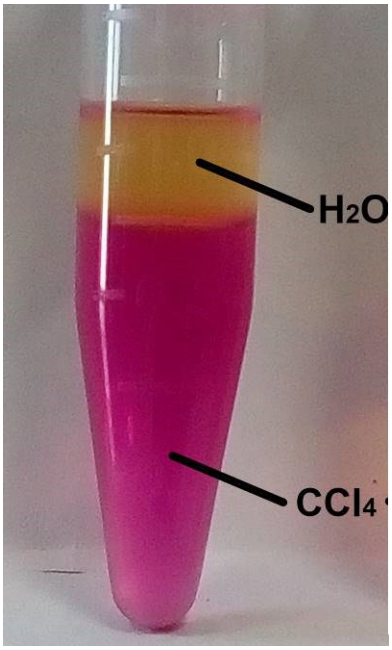

Figure S16 A representative photo of an aqueous solution of salt **5** after adding of a CCl_4 organic solvent.

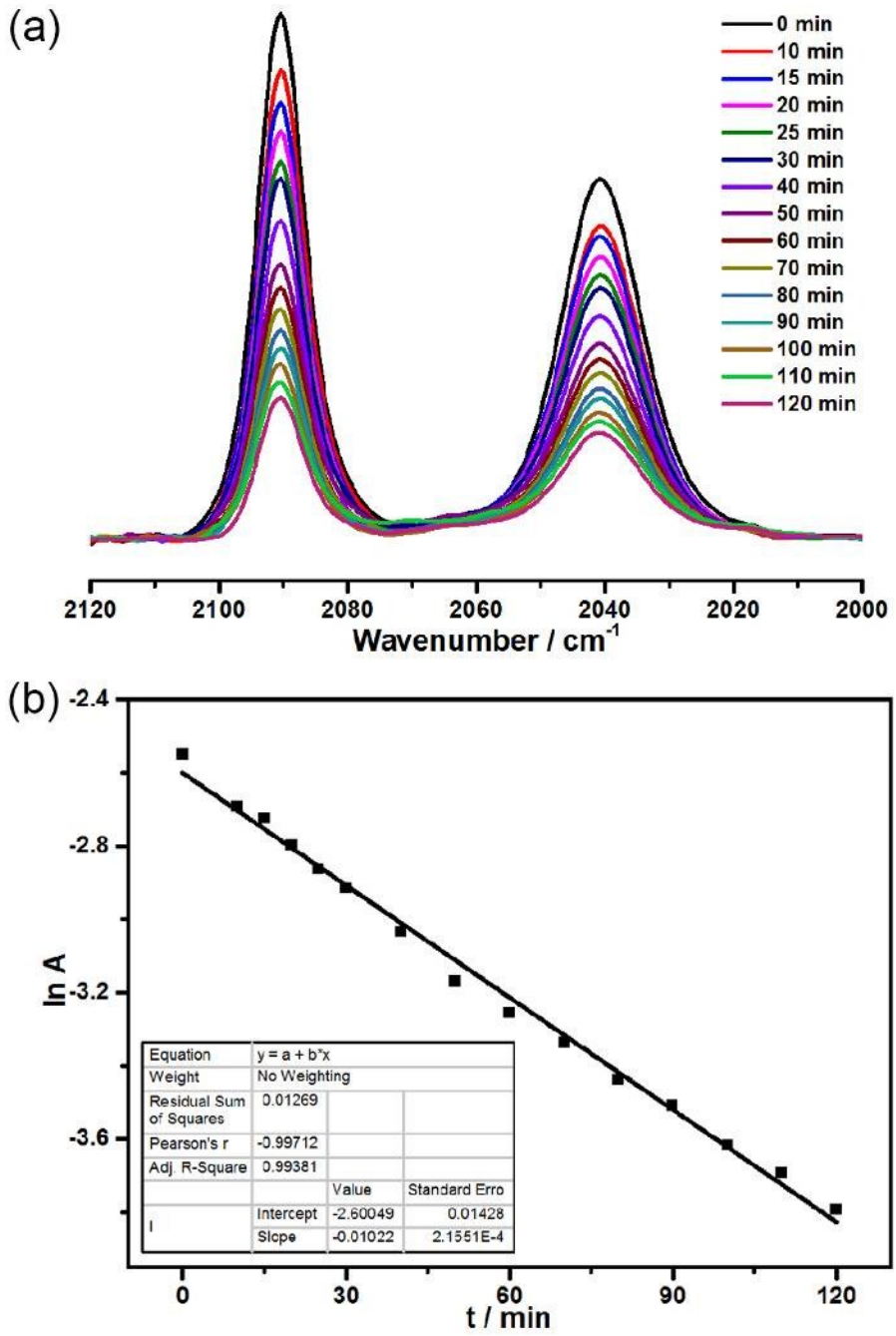

Figure S17 (a) Infrared spectral variation during the CO-releasing process of salt **5** in the present of NaI (0.024 mol L^{-1}) and (b) plot of the vibrational absorption (2090 cm^{-1}) of salt **5** against the process time in D_2O solvent.

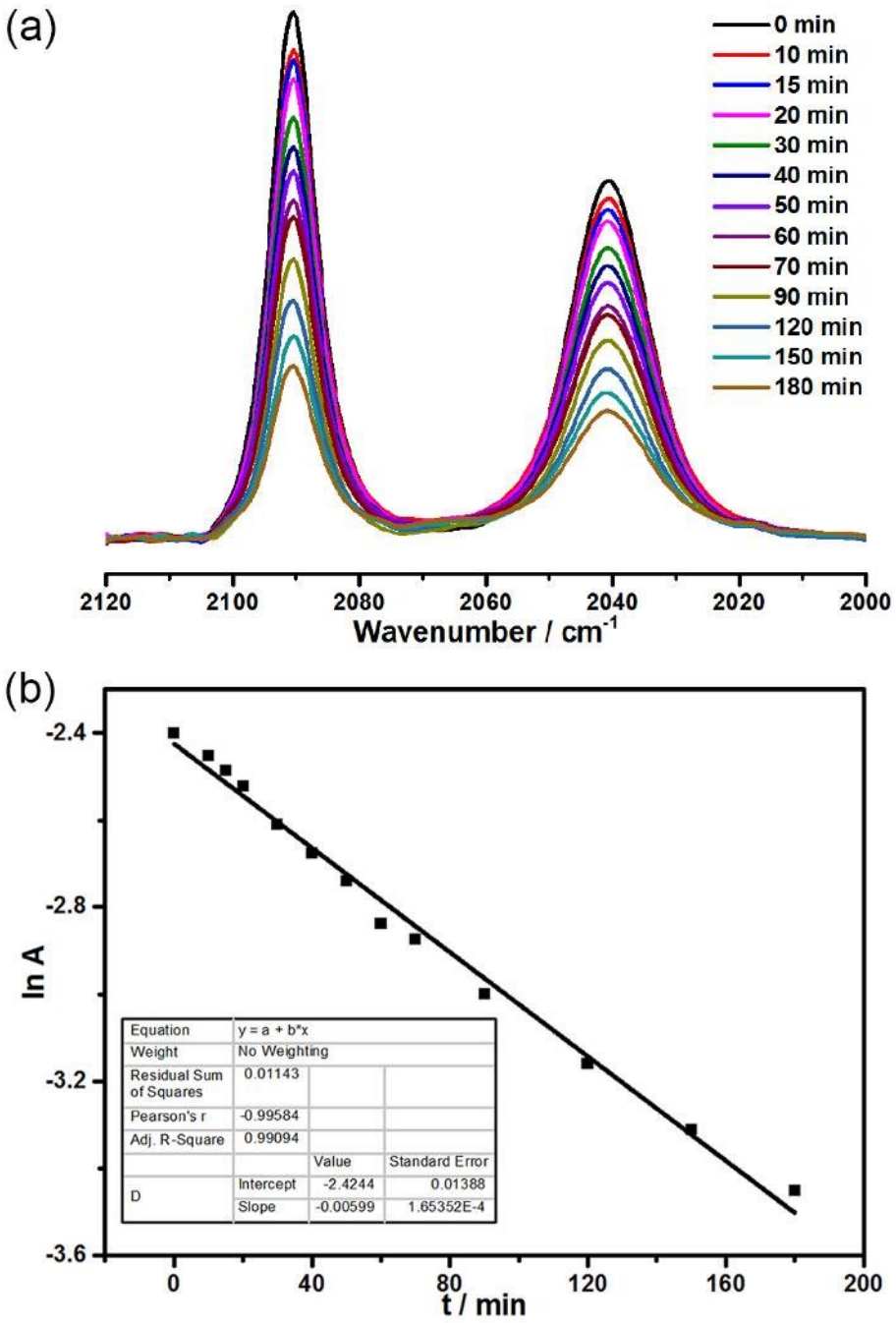

Figure S18 (a) Infrared spectral variation during the CO-releasing process of salt **5** in the present of NaI (0.24 mol L^{-1}) and (b) plot of the vibrational absorption (2090 cm^{-1}) of salt **5** against the process time in D_2O solvent.

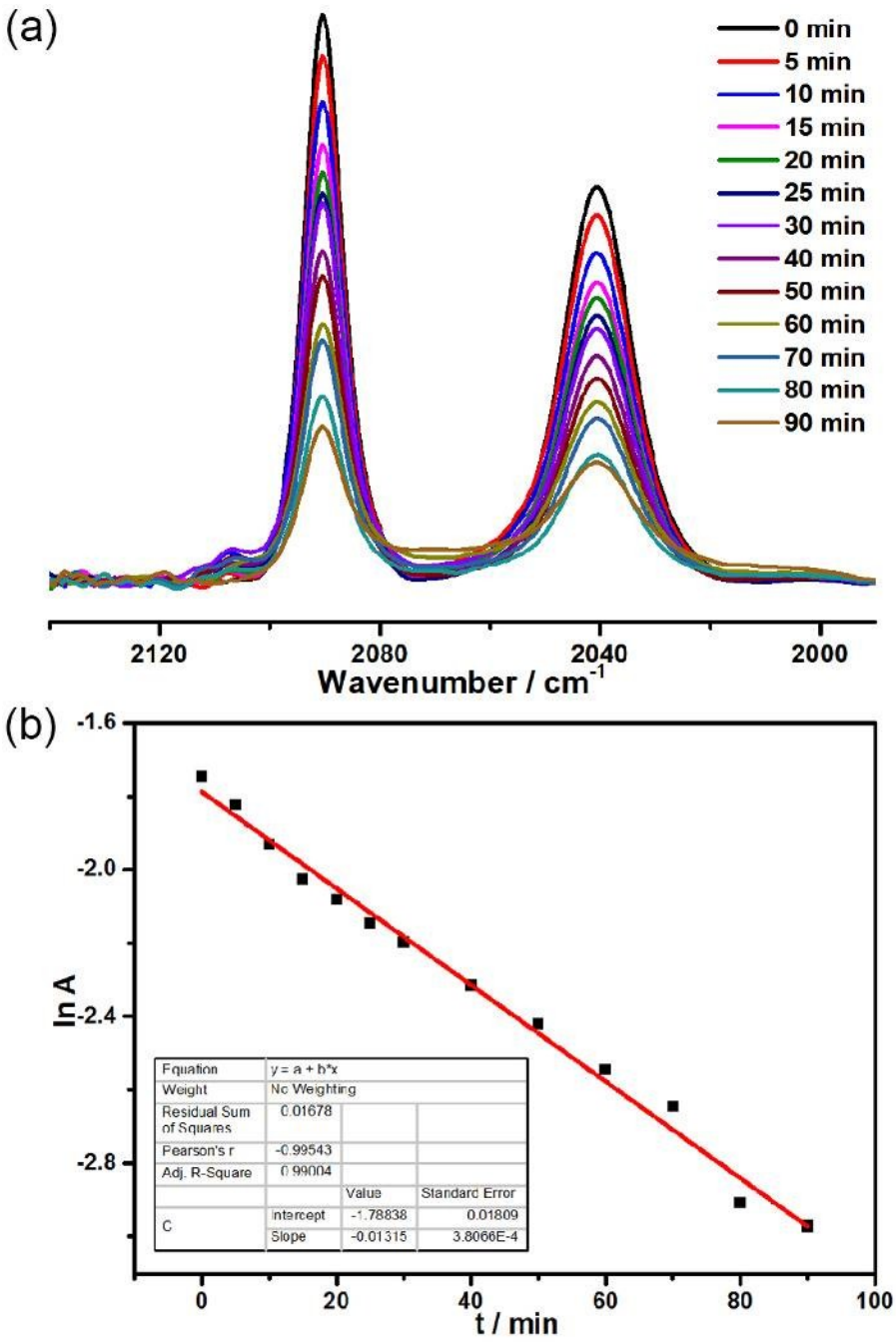

Figure S19 (a) Infrared spectral variation during the CO-releasing process of salt **5** in the present of glucose (0.1 mol L^{-1}) and (b) plot of the vibrational absorption (2090 cm^{-1}) of salt **5** against the process time in D_2O solvent.

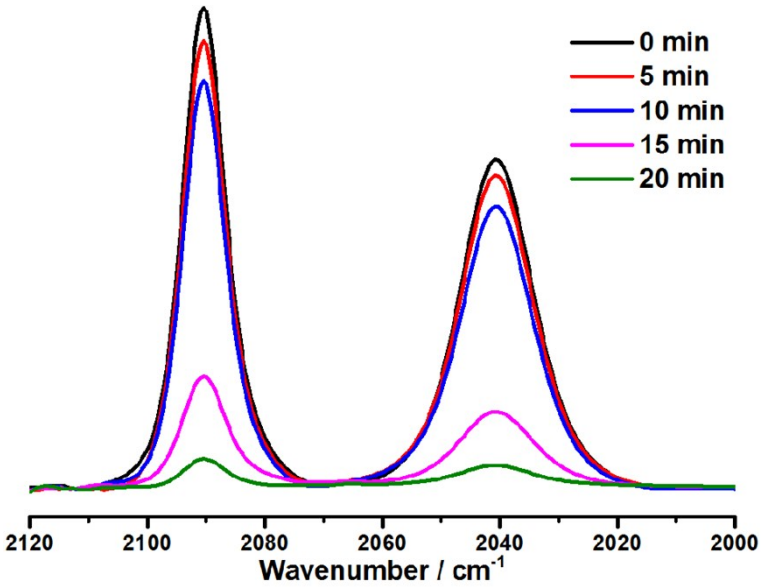

Figure S20 Infrared spectral variation during the CO-releasing process of salt **5** in D_2O solvent under N_2 atmosphere in dark.

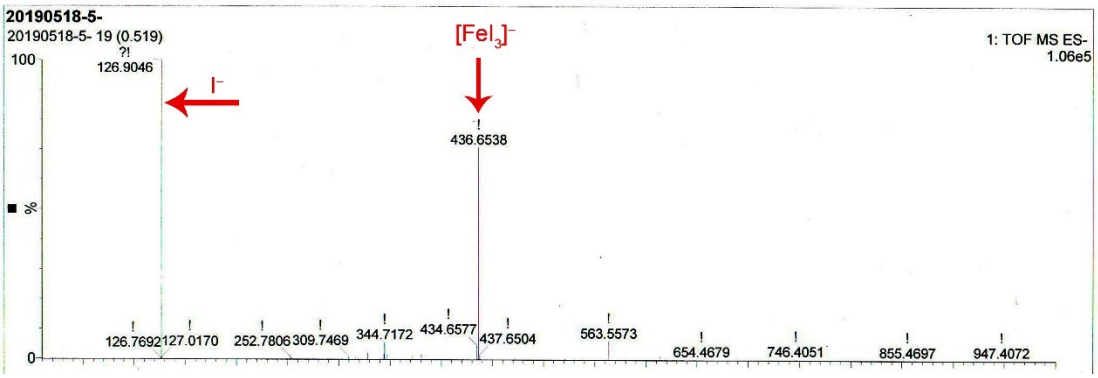

Figure S21 Mass spectrum of i-CORM's solution of salt **5** in D_2O solvent.

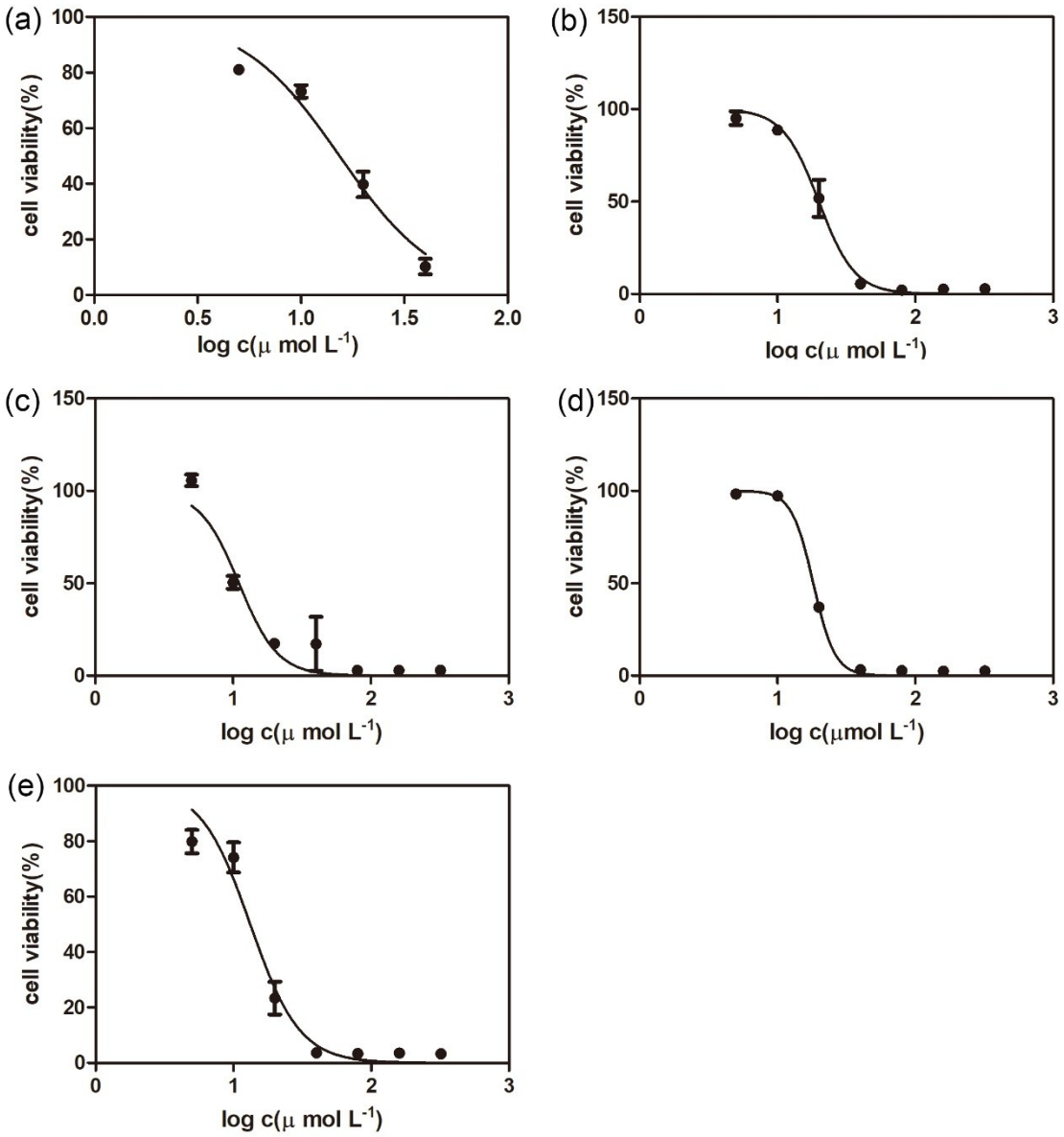

Figure S22 nonlinear regression results of viabilities of RT112 against their responded Logarithm of salt's concentration (log *c*) to estimate IC_{50} values of **1** (a), **2** (b), **3**(c), **4** (d) and **5** (e) in 24 h, respectively.

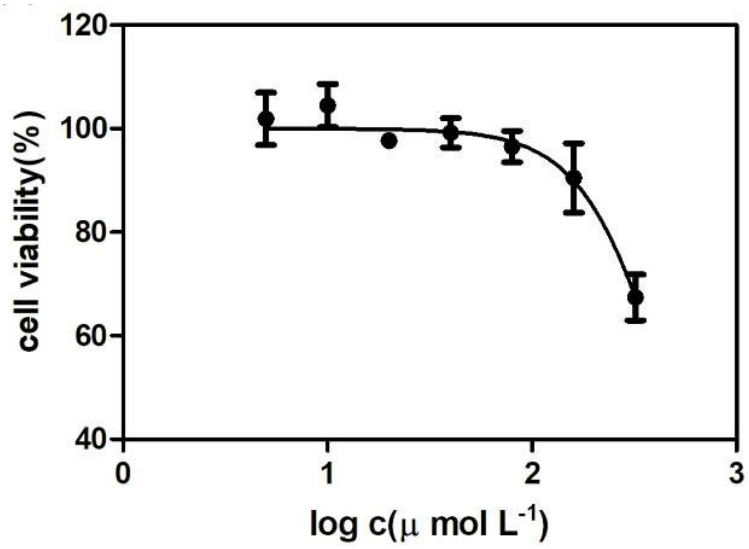

Figure S23 nonlinear regression results of viabilities of RT112 against their responded Logarithm of the i-CORMs' concentration (log *c*) derived from salt **5** to estimate its IC_{50} value in 24 h.

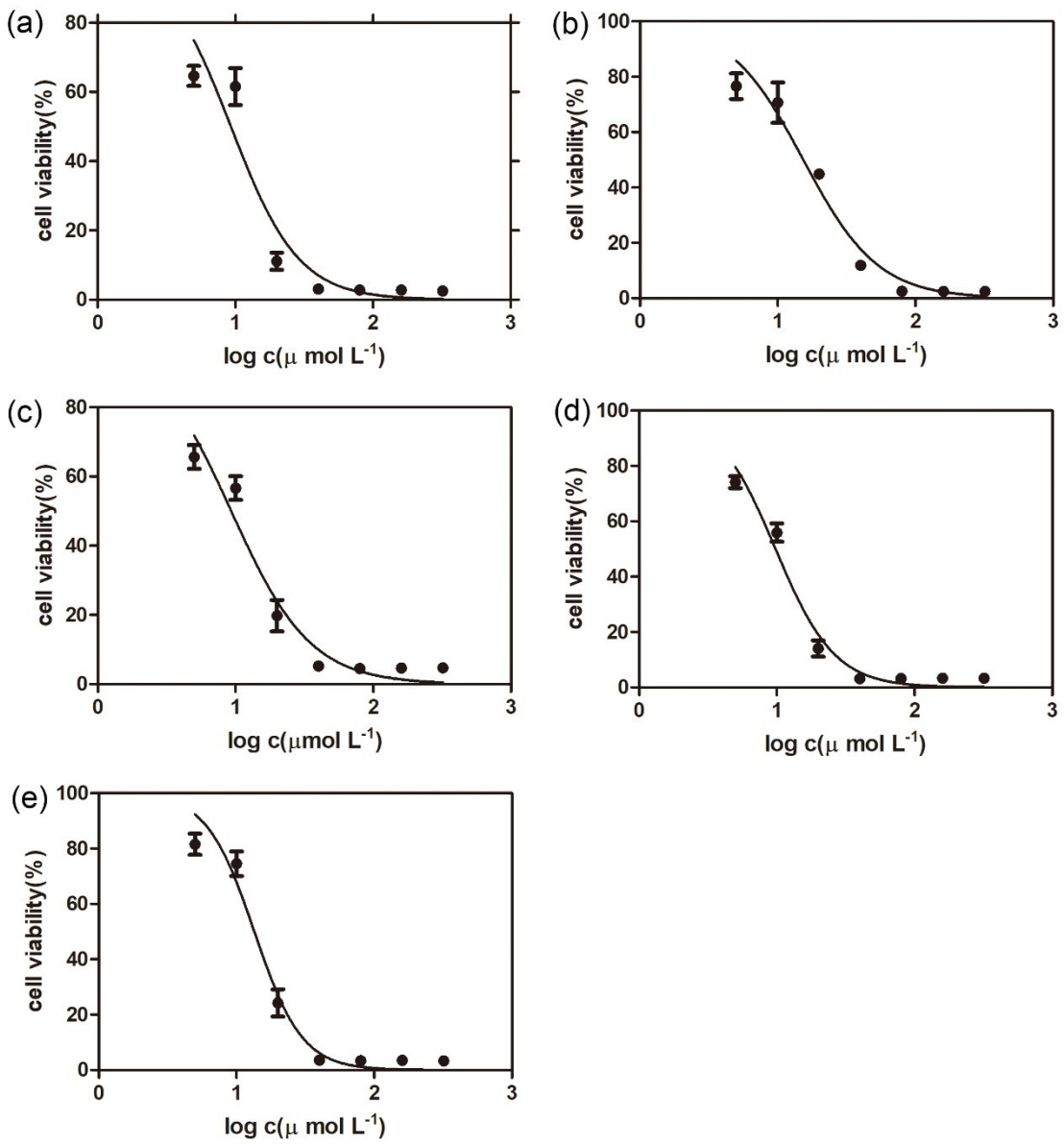

Figure S24 nonlinear regression results of viabilities of SV-HUC-1 against their responded Logarithm of salt's concentration (log *c*) to estimate IC_{50} values of **1** (a), **2**(b), **3** (c), **4** (d) and **5** (e) in 24 h, respectively.

Table S1 Crystal data and structural refinements for salts **1–4**.

	1	**2**	**3**	**4**
CCDC no.	1963446	1963447	1963448	1963449
Formula	$C_5H_8FeI_3NO_3$	$C_6H_{10}FeI_3NO_3$	$C_7H_{12}FeI_3NO_3$	$C_8H_{14}FeI_3NO_3$
Formula weight	566.67	580.70	594.73	608.75
Crystal system	monoclinic	monoclinic	monoclinic	triclinic
Space group	$P2_1/c$	$P2_1/c$	$P2_1/m$	P-1
a/Å	9.2096(8)	12.0358(10)	8.2405(9)	8.092(2)
b/Å	14.5251(12)	7.9704(3)	8.0958(9)	8.2197(8)
c/Å	10.4460(9)	16.4638(10)	12.6129(12)	13.3496(16)
α/°	90	90	90	100.214(9)
β/°	91.739(7)	108.505(8)	106.571(10)	94.639(16)
γ/°	90	90	90	92.457(16)
Volume/Å^3	1396.7(2)	1497.71(18)	806.50(15)	869.5(3)
Z	4	4	2	2
F(000)	1016.0	1048.0	540.0	556.0
2θ/°	5.61 to 59.09	5.738 to 58.634	6.74 to 49.992	5.698 to 49.994
Reflections collected	5969	12199	4931	3010
Independent reflections	3229	3575	1515	3010
Goodness-of-fit on F^2	1.030	1.032	1.040	1.046
R_1, wR_2 (I≥2σ(I))	0.0631, 0.1412	0.0596, 0.0984	0.0572, 0.1447	0.1170, 0.2920
R_1, wR_2 (all data)	0.1131, 0.1687	0.1065, 0.1177	0.0890, 0.1711	0.1625, 0.3462

Table S2 Selected bond lengths (Å) and angles (°) for salts **1–4**.

salt	**1**	**2**	**3**	**4**
Fe1-C1	1.779(16)	1.790(12)	1.758(18)	1.78(2)
Fe1-C2	1.798(16)	1.772(12)	1.762(14)	1.84(3)
Fe1-C3	1.803(15)	1.802(13)	-	1.71(4)
C1-O1	1.106(16)	1.113(12)	1.108(17)	1.08(3)
C2-O2	1.130(16)	1.139(12)	1.139(14)	1.07(3)
C3-O3	1.134(16)	1.082(12)	-	1.20(4)
Fe1-I1	2.6637(19)	2.6431(15)	2.6482(19)	2.648(4)
Fe1-I2	2.6531(19)	2.6425(16)	2.595(8)	2.659(4)
Fe1-I3	2.650(2)	2.6580(15)	-	2.657(4)
Fe1-C1-O1	178.2(15)	178.0(11)	175.4(19)	176(3)
C1-Fe1-C2	94.2(6)	93.7(5)	93.6(6)	93.3(12)
C1-Fe1-I1	179.6(4)	86.1(4)	179.0(6)	86.5(10)
I1-Fe1-I2	93.00(6)	93.70(5)	94.8(3)	93.61(13)